Electrical Characteristics of Au-Al and Cu-Al Intermetallic Compounds in Thermosonic Interconnection Interface

T Joseph Sahaya Anand[1,*], Lee Wen Hau[1], Chua Kok Yau[1], Ong Sai Boon[2], D. Ranjith Kumar[3]

[1]Department of Engineering Materials, Faculty of Manufacturing Engineering, Universiti Teknikal Malaysia Melaka (UTeM), 76100 Durian Tunggal, Melaka, Malaysia

[2]Infineon Technology (Malaysia) Sdn. Bhd., FTZ Batu Berendam, 75350 Melaka, Malaysia.

3Department of Nanoscience and Technology, Bharathiar University, Coimbatore, 641046, India.

*corresponding author: anand@utem.edu.my

Abstract: In this report, the electrical resistance of the intermetallic compounds (R_{IMC}) at bonding interfaces of gold (Au)- and copper (Cu)-aluminum (Al) in a microchip was studied. Micro-structural and electrical characterizations were performed on the samples prepared with combinations of wire types, bonding temperatures and High Temperature Storage conditions. It was observed that the IMC growth was generally in the parabolic manner which implied the volume diffusion mechanism. The resistance of the interfacial intermetallic compound (IMC), R_{IMC} was related to High Temperature Storage (HTS) duration, t, in the exponential manner due to void formation. This contributed to the exponential correlation between the R_{IMC} and IMC thickness. This contravened the common observation of a linear relationship between the resistance of IMC and its thickness. Furthermore, a theoretical model was developed to predict the bonding interfacial contact area. The contact area was calculated from measurements of concentration profile, IMC thickness and electrical resistance. It was anticipated that the interfacial contact area varies with the IMC thickness in a "bell-shape" manner. The predicted contact area and its diameter, based on cylindrical geometry, were in a good agreement to that of experimental measurement.

1. INTRODUCTION

In microelectronics packaging industry, thermosonic wire bonding has been an important assembly technique. It enables the electronic interconnection from bond pads of an integrated circuit (IC) to an external substrate or lead frame via bonded wires [1]. Kim et al claims that thermosonic wire bonding has been used for its advantage of better stability and cost effectiveness despite the current trend of flip chip interconnection on high inputs/outputs (I/Os) and high-speed devices [2].

Thermosonic Gold (Au) wire bonding on Aluminum (Al) bond pad metallization has been a common electrical interconnection employed in the microelectronics industry. Au wire bonding offers plenty of benefits: self-cleaning, high yield, flexibility and reliability [3]. Nowadays, Copper (Cu) interconnection technology has grown interested in the industry, mainly due to a lower cost and enhancement of the reliability of components [4–6].

Studies of intermetallic compound (IMC) at both Au and Cu wire-Al bond pad interface (Au-Al and Cu-Al) has been the major research direction performed by many researchers [2,4–6]. This is crucial as IMC is believed to contribute to failures at the wire bonding interface. In general, a sufficient growth of IMC under High Temperature Storage (HTS), which is an industrial standard isothermal annealing process, improves the bondability. However, an excessive growth of IMC could lead to a degradation of reliability of the bonding due to the formation of voids and increase of electrical resistance [2,7,8]. Moreover, the electrical resistances of Cu-Al IMCs are lower than that of Au-Al [1] indicates that the devices with Cu wires bonded have better performance. Besides, it

is commonly observed that the growth of both Au-Al and Cu-Al system complies to a parabolic behavior [9–11] which reflects the nature of the volume diffusion mechanism [12].

On the other hand, the study of electrical characteristics of IMC that present at the bonding interface is less common compared to microstructural studies. Braunovic et al reports that IMC formation at the interface of Cu-Al metal couple induces a contact resistance. The contact resistance change increases with the thickness of IMC in a linear manner [13]. A similar linear behavior but with a greater slope is seen in the works of Wei et al [14] that focuses on the contact resistance analysis of the micro-electronic device with Au and Cu wired Al-1%Si bond pad. This is explained by the electrical characteristics of Cu-Al systems with different dimensions. In addition, another report from the similar research group [15], it is generally observed that the contact resistance of Cu-Al IMC increases slowly with the annealing duration up to 1000 hours. On the other hand, the Au-Al contact resistance shows a tremendous increment. One may notice that the electrical characterization is less performed on the pure Al bond pad of the microchip, perhaps alloyed Al bond pad which improves the electromigration resistance [16] is more favorable for product stability. Moreover, samples of mentioned studies are believed to be fabricated with a constant wire bonding temperature. Thus, the effect of bonding temperatures towards IMC growth under HTS and electrical characteristic change is not properly evaluated before.

The objective of the present study focuses on the microstructural and resistance analysis of the IMC developed at the bonding interface of wire-Al bond pad. Experimental variables considered were wire materials, bonding temperatures and HTS durations. The correlation between the IMC growth and resistance of the IMC is evaluated.

2. EXPERIMENTAL PROCEDURES

The sample fabrication was started with die bonding process to transfer microchip from wafer form to leadframe. Then the Thermosonic wire bonding process was carried out to interconnect wires on the Al bond pad and leadframe. Process parameters and equipments used in the sample synthesis were similar to that of [17], except that sample were bonded with both Au and Cu wires, bonding temperatures employed were 280 and 400°C. Bonded samples were then further proceed with molding, galvanic tin (Sn) plating, trim/form and finally electrical testing. Tested functional samples were then loaded into the HTS oven for annealing at 175°C up to 1000 hours with a duration interval of 100 hours. Then a cold mounting was performed prior to the cross-sectional grinding and polishing to expose the center of Au/Cu-Al bonding interface. The microstructural characterization of IMC at the bonding interface was performed using Zeiss Axioskop 2 MAT Optical Microscope (OM). Selected samples were inspected using JEOL-LV/EDX Scanning Electron Microscope (SEM) with Energy Dispersive X-ray (EDX). Besides, the as-bonded sample was selected and prepared with Focused Ion Beam (FIB) for Transmission Electron Microscopic (TEM)/EDX analysis. The lamella was extracted from the periphery of the ball bond (high stress area) and transferred to a Molybdenum (Mo) grid before TEM/EDX analysis.

As for the electrical resistance of the IMC, it was determined from the following equation:

$$R_{IMC} = R_d - R_c - R_L - R_W \quad (1)$$

Where

R_{IMC} = Resistance of IMC layer present at the bonding interface of a diode device (Ω),

R_d = Measurement of resistance of a diode device which obtained from V-I characteristic (Ω),

R_c = Measurement of resistance of the diode chip (Ω),

R_L = Measurement of resistance of leadframe (Ω),

R_W = Measurement of resistance of wire in the device (Ω),

R_d was measured using Sony/Tektronix 370A Programmable Curve Tracer curve tracer. R_c, R_L and R_W were measured with Kevin's Double Bridge which is meant for small resistance measurement [18]. It was convenient to perform the resistance measurements of R_c and R_L together as their had been bonded. Moreover, it was difficult to measure R_w directly from the bonded wires due to their short

length in a unit of wire bonded microchip. Thus, R_w was estimated by first measuring the resistance of the wires with a reasonable length (e.g. 30cm). Then R_w could be estimated by calculating the ratio of the total wire length in a unit of microchip (about 0.65mm) to 30cm and multiply the measured resistance of the wire with 30cm.

From measurements, it was estimated that

$$R_c + R_L \approx 1.824\ m\Omega \qquad (2)$$

$$R_W \approx \begin{cases} 0.122\ \mu\Omega \text{ for Cu wire} \\ 0.146\ \mu\Omega \text{ for Au wire} \end{cases} \qquad (3)$$

Equation (1) could be written in approximate manner as

$$R_{IMC} \approx R_d - 1.824 \qquad (4)$$

3. RESULTS AND DISCUSSION

The OM inspection on the IMC thickness for both Au and Cu wire samples that were prepared with various combinations of bonding temperatures and HTS conditions was carried out. Figure 1a to c show the thickness measurement results of different wire-bonding temperatures-HTS condition systems. It was observed that the higher bonding temperature generated a higher initial IMC thickness, i.e. from about 0.49µm at 280°C to 0.71µm at 400°C. However, the IMC thickness after HTS treatment was strongly affected by HTS temperature and durations. The parabolic trend of the IMC thickness (x) with HTS durations (t) was visually observed in Figure 1a, however, this trend was not obviously seen in Figure 1b and c. A linear regression analysis on x2 versus t plot is helpful for confirming whether the parabolic trend existed in the IMC thickness measurements of other samples [19]. Figure 2 shows the results of the regression analysis. Values of coefficient of determination (R2) of each category of sample labelled in Figure 2 were found greater than 0.80. This indicated a strong linear correlation between x2 and t. Therefore, the parabolic trend of IMC growth kinetic for sample evaluated was evident. This leads to an implication that the IMC development at the bonding interface is controlled by volume diffusion [11,20]. The similar phenomenon was reported in other reports [1,7].

Measurements of RIMC of both Au and Cu bonded samples with HTS temperatures of 175 and 200°C were shown in Figure 3a and b, respectively. Generally, RIMC increased with HTS durations in an exponential manner. This indicated a degradation of conductivity of the bonding interface over the HTS duration. Moreover, with HTS at 175°C, the magnitudes of measured RIMC were in the order of Au wire sample (synthesized at 280°C) > Cu wire sample synthesized at 400°C > Cu wire sample synthesized at 280°C. However, for samples annealed at the higher HTS temperature (200°C), RIMC of samples bonded with Cu wire were greater than that of Au wire sample. Changes in RIMC were explained through the IMC development or thickening and void formation at bonding interface. A growth in the thickness of a Cu-Al or Au-Al IMC naturally results in an increase of interfacial resistance. This is due to the resistivities of these IMCs are greater than that of pure Cu, Au and Al metals [1]. Moreover, the formation of voids at the bonding interface reduces the contact area between Cu/Au and Al. This again leads to an increase of the interfacial resistance.

At the lower HTS temperature, the trend of RIMC measurements was controlled by the IMC growth at the bonding interface. A rapid growth of Au-Al IMC (refer Figure 1a) resulted in a greater RIMC. Likewise, the IMC thickness of the Cu wire sample synthesized at 400°C was relatively higher than that of similar sample prepared at 280°C. Besides, the trend of RIMC of Au wire sample and Cu wire sample with bonding temperature of 400°C were noticed to deviate from a linear manner after 700 hours of HTS treatment. This was due to initiation of void formation at the bonding interface. For the Au wire sample, it is generally known that the Au-Al IMC and void formation are rapidly developed at the bonding interface [21,22]. This phenomenon was observed in image of optical microscope (OM) as shown in Figure 4a. This explained the most deviated RIMC-HTS duration pattern from a linearity as seen in Figure 3a. For Cu wire samples, similar failure analysis using an OM is not feasible due to limitations in its magnification. Instead, Scanning Electron Microscope is necessary. Figure 4b and c show the comparison of FESEM images of cross-sections of Cu wire samples synthesized at both 280 and 400°C, respectively, after 175°C HTS for 1000 hours. It was observed that small voids formation at the bonding interface was found only in Figure 4c. This explained the intermediate deviation of the RIMC-HTS duration pattern for Cu wire sample synthesized at 400°C. There was no observation of the void formation at the bonding interface in Figure 4b. This resulted in the RIMC-HTS duration pattern with almost no deviation from linearity.

From Figure 3b, after HTS treatment at 200°C, RIMC of the Cu wire samples at the HTS temperature of 200°C was found greater than that of Au wire sample. It was strongly believed that the void formation at the bonding interface was prominent in affecting RIMC rather than the IMC growth or thickening. This was due to the growth of Cu-Al IMC that is much slower than that of Au-Al ([1,2] and Figure 1). This was supported by the magnified OM images of both Au and Cu wire samples as shown in Figure 5 which revealed different levels of void formations at the bonding interfaces. It was observed that the magnitudes of voidings were in the order of Au wire

sample < Cu wire sample synthesized at 280°C < Cu wire sample synthesized at 400°C. This explained the trend of RIMC measurements as seen in Figure 3b.

Figure 6 shows the linear regression analysis of plots of ln(RIMC) versus HTS durations (t, in the unit of hours). Empirical linear equations of each category of sample and their corresponded coefficient of determinations (R2) were labelled in Figure 6. From the values of R2 > 0.8, ln(RIMC) established a strong linear correlation with t. In other words, the exponential correlation between RIMC and t was proven statistically. According to Wei et al [15], an exponential increasing trend of contact resistance with HTS duration is graphically observed for 50µm Au wire bonded on Al-1%Si sample after 150°C HTS treatment. However, this observation is not further analyzed and confirmed. The exponential growth of RIMC with HTS durations as observed in this study was the major reason that caused the exponential relationship between RIMC and IMC thickness as discussed in following.

Empirical and regression result could be summarized into following equations:

a. From the empirical results of IMC thickness, x after HTS duration of t, [9]

$$x - x_0 = A\sqrt{t} \quad (5)$$

b. From the empirical results of R_{IMC} after HTS duration of *t*

$$R_{IMC} = Be^{Ct} \quad (6)$$

From (5) and (6),

$$R_{IMC} = Be^{D(x-x_0)^2} \quad (7)$$

Where A, B, C and D were constants that had S.I. units of $ms^{-1/2}$, Ω, s^{-1} and m^{-2}, respectively. x_0 was the thickness of IMC at t = 0. It was noted that A described the increment rate of IMC thickness after HTS, B was corresponding to the initial R_{IMC}, C and D were the exponents which determined how rapid the R_{IMC} change with *t* and the $(x\text{-}x_0)$, respectively. Table 1 summarizes the estimated values of these quantities from the experiment.

Equation (7) was validated by plotting $\ln R_{IMC}$ versus $(x\text{-}x_0)^2$. Then a linear regression analysis was performed and summarized in Figure 6 and Figure 7 for Cu and Au wire samples, respectively. The corresponding linear equations and R^2 values were labelled in these plots. Strong linear correlations were observed and thus the relationship in equation (7) was valid. The exponential relationship as observed in this experiment was contracting the common observation by other researchers. According to [13] which studies on friction welded Al-Cu bimetal, difference of resistance around the joint (before and after heat treatment) is proportional to IMC thickness. Wei et al reports the similar linear relationship on Cu wire bonded Al-1%Si bond pad sample [15]. The similar conclusion is made in [23] that studies the IMC in cold rolled Cu-Al bi-metal. However, measurement data in this study could hardly fit this linear relationship statistically.

It is possible to estimate the contact area of Cu-Al based on the measurement of the electrical resistance and IMC thickness through the following equation:

$$Interfacial\ contact\ area,\ I = \rho\frac{x}{R_{IMC}} \quad (8)$$

Where

ρ = resistivity of the IMC formed at the bonding interface (S.I. unit: Ωm),

x = IMC thickness,

R_{IMC} = electrical resistance.

It was noted that by substituting equations (7) into (8) while treated ρ as a constant, equation (8) became

$$I = \frac{\rho}{B}e^{-E(x-x_0)^2} \quad (9)$$

he corresponding plot of I versus x based on equation (9) will be in the form of a symmetrical bell-shape as shown in Figure 8. This meant that *I* increased with the IMC thickness until a critical thickness which *I* reached its maximum value. Then *I* started to reduce when the IMC thickness was further thickened. In fact, this bell-shape behavior was upheld for any function of ρ, except when it was in an exponential form in term of *x* that cancelled the similar exponential component in Equation (9). This subsequently resulted in a constant *I*. The reduced trend of *I* was again due to void formation at the bonding interface which resulted in the exponential relationship between R_{IMC} and *x* (equation (7)).

Value of x and ρ can be determined from compositional analysis e.g. EDX line scan. ρ is determined by recognizing the phase exist at the Cu-Al interface according to the composition in this region using phase diagram. For single phase system, ρ is a constant and equation (8) could be used directly. However, for a binary phase system which the concentration of elements falls between two phases in the phase diagram, ρ in equation (8) comply the following relationship [24]:

$$\rho = \rho_\alpha V_\alpha + \rho_\beta V_\beta \quad (10)$$

where

V_α and V_β are volume fraction of α- and β-phase which exist at the bonding interface, respectively. ρ_α and ρ_β are electrical resistivity of α- and β-phase, respectively.

Equation (9) can be further expanded and written in term of the mass-fraction of each phase, concentration measurement of one of the elements (e.g. Cu) and mass-density of the elements [25]:

$$\rho = \rho_\alpha + \frac{\rho_\beta - \rho_\alpha}{1+\left(\frac{c_\beta - c}{c - c_\alpha}\right)\left(\frac{\rho_\beta}{\rho_\alpha}\right)} \quad (11)$$

where

c = measured concentration of Cu element using line scan EDX, with $c_\alpha < c < c_\beta$. c_α and c_β are the concentrations of Cu element at which a tie line at low temperature (<300°C) [26] intersects with the α- and β-phase boundary lines. P_α and P_β are the mass densities of α- and β-phase, respectively.

Combinations of the equations (9) and (11) enable the estimation of the contact area at the bonding interface after the HTS process, if a similar compositional analysis can be done on annealed samples. In this work, however, only the as-synthesized Cu wire bonded sample prepared with the bonding temperature of 280°C was assessed with TEM and line scan EDX analysis. The analysis was performed at the periphery of the ball bond (high stress area) and the result was shown in Figure 9a and b. Figure 9a was the imaging result at the high stress area and a red line in the image indicates the position of the line scan EDX measurement. Figure 9b was the composition profile of both Cu and Al element along the scanning line. From Figure 9b, it was determined that the thickness of the IMC layer ~350nm and the average Cu concentration at the bonding interface ~57 wt%. OM is out of capability to assess this IMC thickness. From the equilibrium phase diagram [26], there was a layer of mixture of $CuAl_2$ (θ, as α-phase) and CuAl (η_2, as β-phase) phases at the bonding interface. From literature, following key variables are determined: $\rho_\alpha = \rho_\theta = 8\mu\Omega cm$, $\rho_\beta = \rho_{\eta 2} = 11.4\mu\Omega cm$ [27], $c_{CuAl_2} = 54.04 wt\%\ Cu$, $c_{CuAl} = 70.20 wt\%$ [12], $P_{CuAl_2} = 4349.5 kgm^{-3}$ and $P_{CuAl} = 5131.0 kgm^{-3}$ [28]. These data resulted in an estimated resistivity of the mixture of phases at the bonding interface of 8.54μΩcm from Equation (11). Then the contact area was predicted using equation (9), i.e. 2040μm^2. With an assumption that the development of IMC at the bonding interface was ideally a cylinder with thickness of ~350nm, then the expected diameter of the contact ~50μm. Figure 9c show the magnified cross-sectional OM image of the ball bond of the as-synthesized Cu wire sample. It was observed that the contact area was with a diameter of about 40μm. Therefore, the estimated value of contact diameter was rather accurate. This method used measurements of the electrical resistance, IMC thickness and concentration profile of one of the elements at the bonding interface to estimate the interfacial contact area. This contact area measurement technique could be a complement to a common mechanical cross-section technique and an effective alternative to time consuming "slice-and-view" FIB/SEM method [29,30].

4. Conclusion

Measurements of the IMC thickness and R_{IMC} of samples prepared with various wire types, bonding temperatures and HTS conditions were performed. It was observed that the IMC thicknesses complied to the parabolic rule. This implied that the growth of the IMC was dominated by the volume diffusion mechanism. The exponential increase of R_{IMC} with HTS durations was due to the void formation at the bonding interface. This was evident in the SEM analysis of the annealed Au and Cu wire samples. This led to an exponential increase of R_{IMC} with IMC thickness. This observation was unique as other reports claim a linear correlation between these quantities. The exponential behavior of R_{IMC} further impacted in the modeling of the interfacial contact area of the bonding interface. It was predicted that the contact area increased with IMC thickness initially. When a critical thickness was reached, the contact area was maximized. However, the contact area decreased when the IMC thickness was further thickened. This behavior was generally upheld, except in the case that the electrical resistivity was an exponential function in term of IMC thickness. This resulted in the cancellation of the exponential component in the equation of R_{IMC}. This subsequently caused *I* a constant value. Furthermore, a theoretical model of the interfacial contact area was developed. This model enabled the estimation of the contact area from the concentration profile, IMC thickness and electrical resistance. It was estimated that the interfacial contact area ~2040μm^2 or diameter of the contact ~50μm which was in a good agreement with the optical microscopic observation.

Table 1: Summary of IMC growth and R_{IMC} increment related quantities.

Wire type	Bonding Temperature (°C)	HTS temperature (°C)	A (10^{-3} μm/hr$^{1/2}$)	B (10^{-3} mΩ)	C (10^{-3} hour^{-1})	D (10^{-3} m^{-2})
Au	280	175	167.063	33.507	2.256	2.256
Au	280	200	197.687	30.107	2.962	2.962
Cu	280	175	30.047	17.583	1.872	1.872
Cu	280	200	35.256	16.472	4.807	4.807
Cu	400	175	24.950	27.087	2.145	2.145
Cu	400	200	30.030	31.575	4.512	4.512

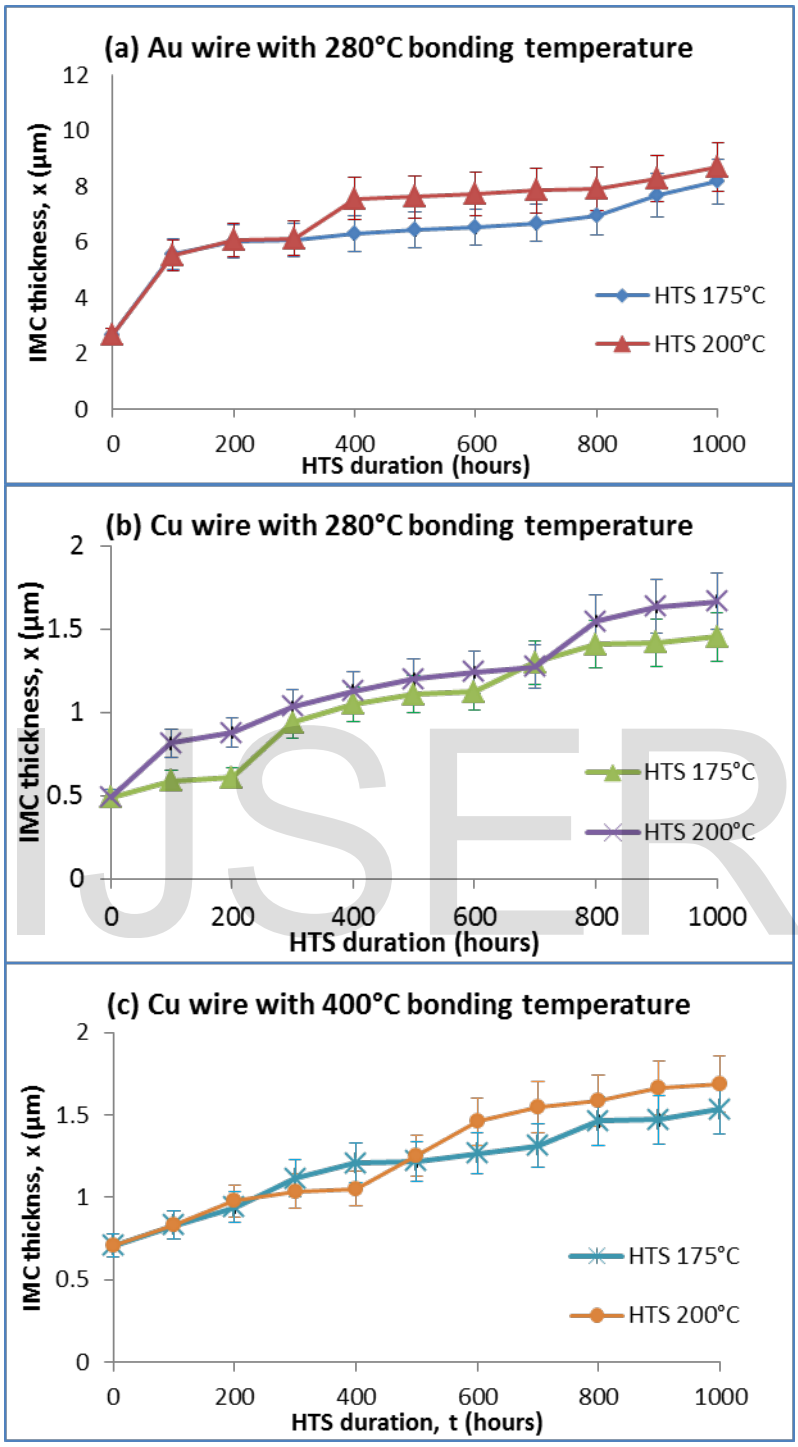

Figure 1: Results of IMC thickness versus HTS duration in for (a) Au wire wired sample synthesized at 280°C, (b) Cu wired samples synthesized at 280°C, (c) Cu wired samples synthesized at 400°C.

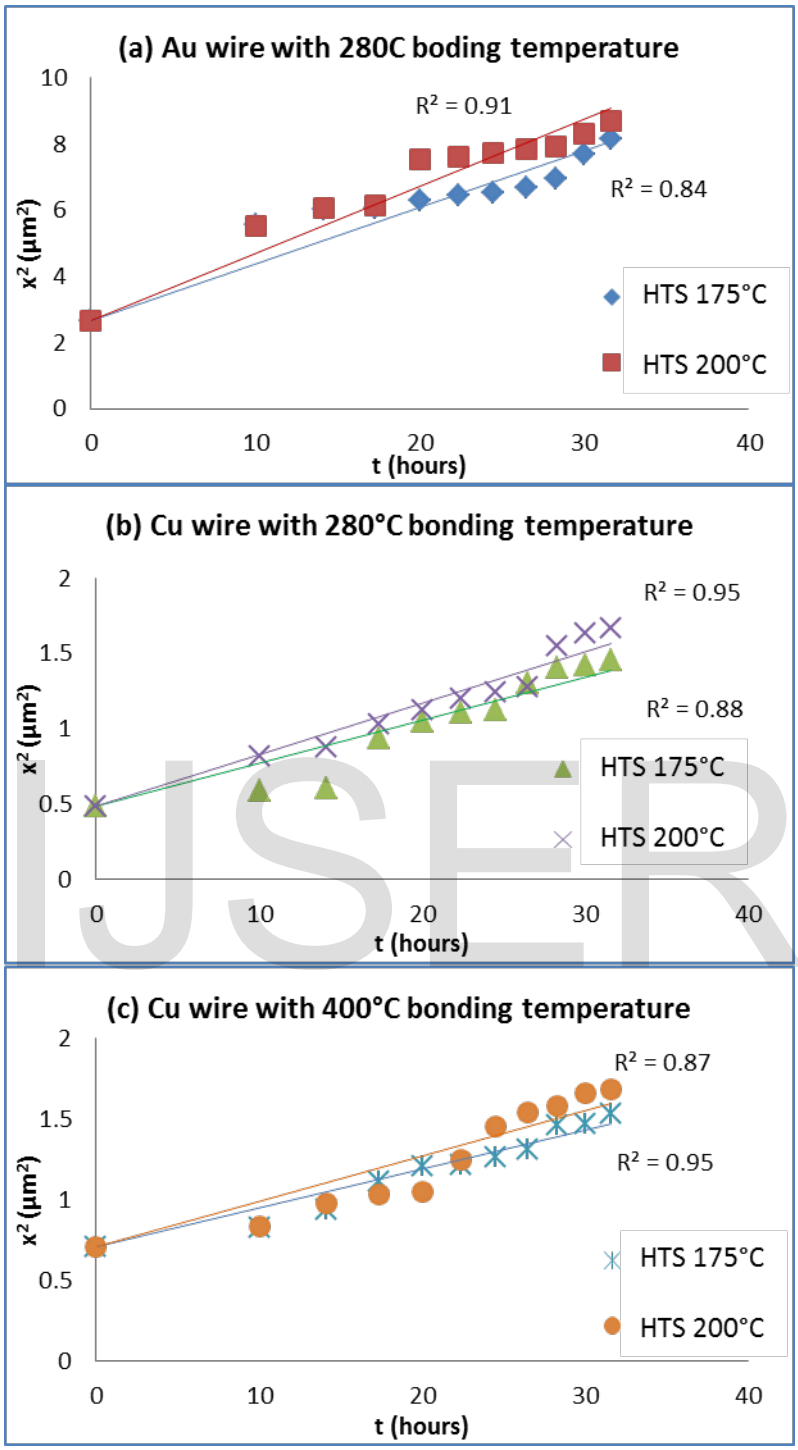

Figure 2: Results of linear regression analysis (x^2 vs t) for various wire materials-bonding temperatures combinations: (a) Au-280°C, (b) Cu-280°C and (c) Cu-400°C.

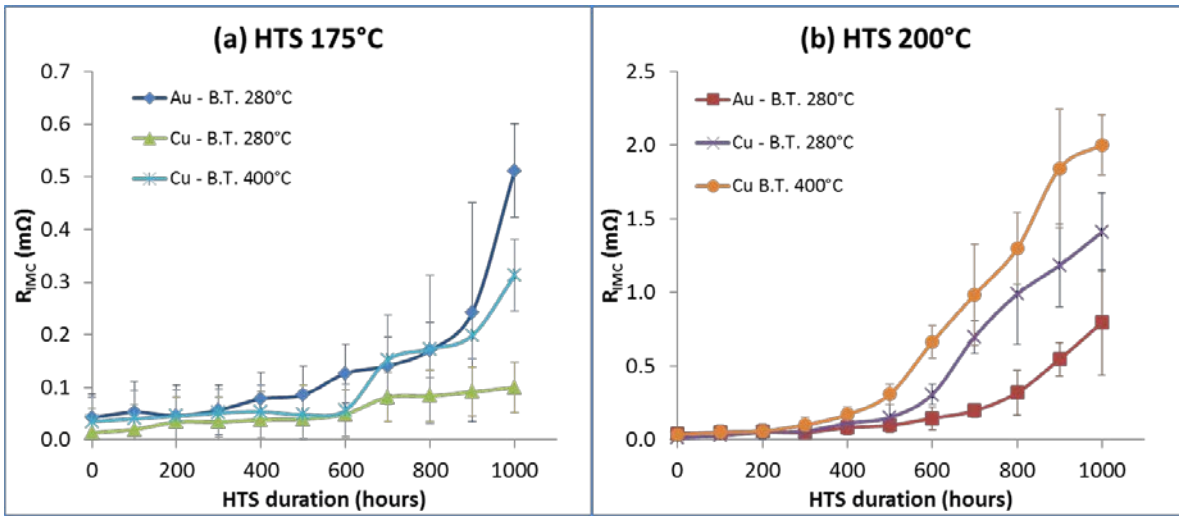

Figure 3: (a) measurement of R_{IMC} for both Au and Cu wire sample with different bonding temperatures and HTS conditions. (b) was the result of regression analysis of (a).

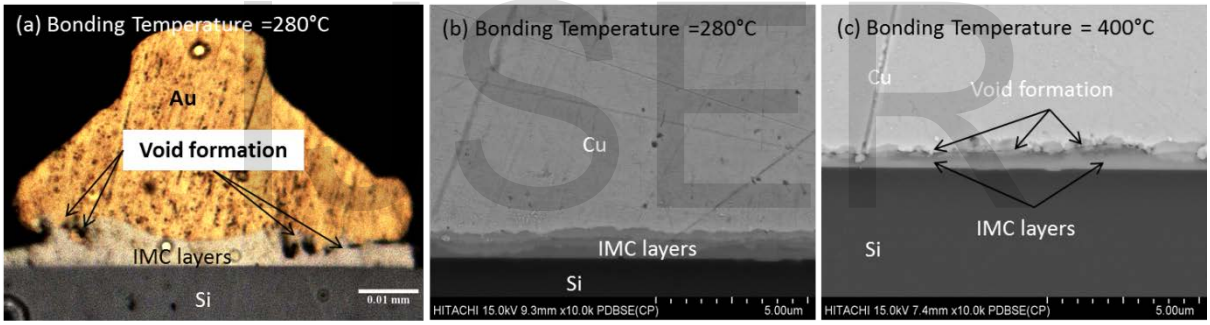

Figure 4: (a) Optical micrograph of Au wire samples after 1000 hours of HTS at 175°C. FESEM results on cross-sectioned samples of Cu wire samples after HTS 1000 hours at 175°C that were synthesized at (b) 280 and (c) 400°C.

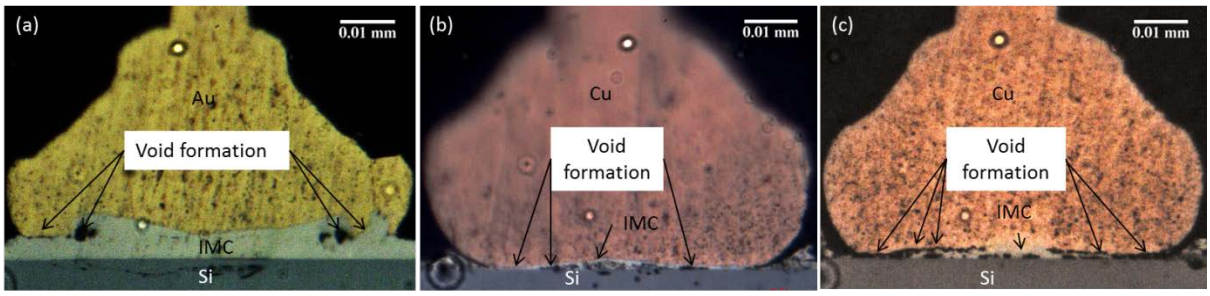

Figure 5: Optical micrograph of (a) Au wire sample, Cu wire sample synthesized at (b) 280°C and (c) 400°C, after 1000 hours of HTS at 200°C.

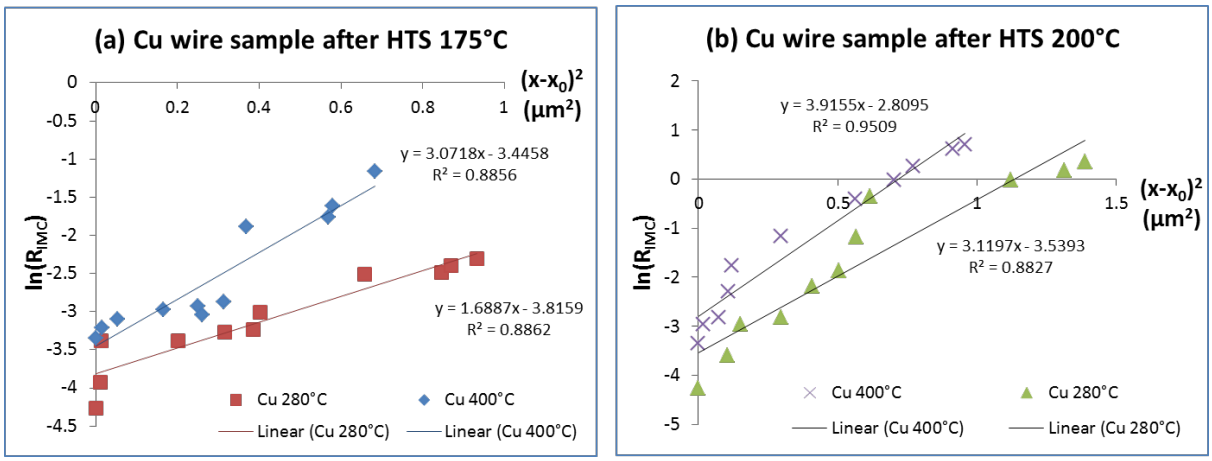

Figure 6: Linear regression analysis on Cu wire samples annealed in HTS temperature of (a) 175 and (b) 200°C. Values specified in legends were referring to bonding temperatures.

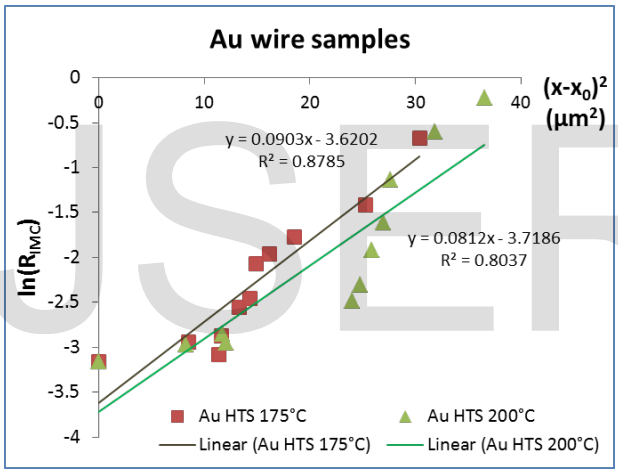

Figure 7: Linear regression analysis of Au wire samples.

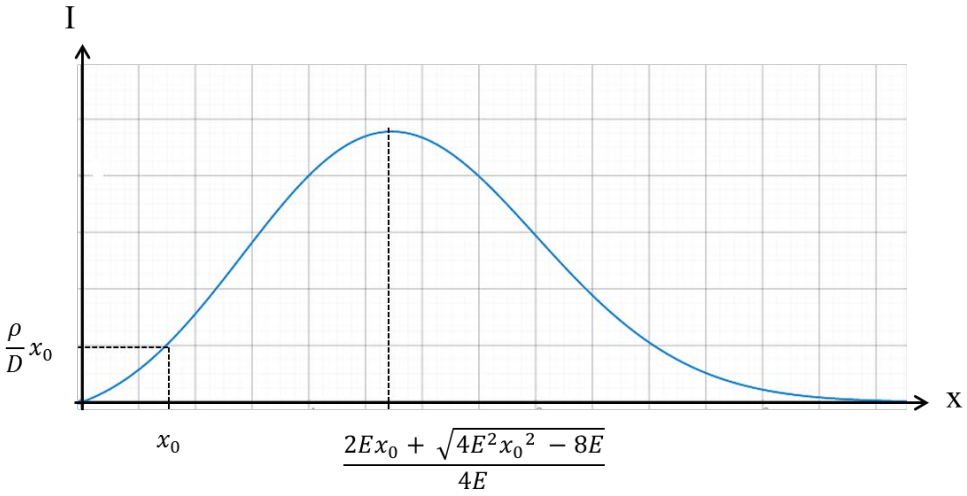

Figure 8: Plot of I versus x based on equations (7) and (8) by assuming ρ was a constant.

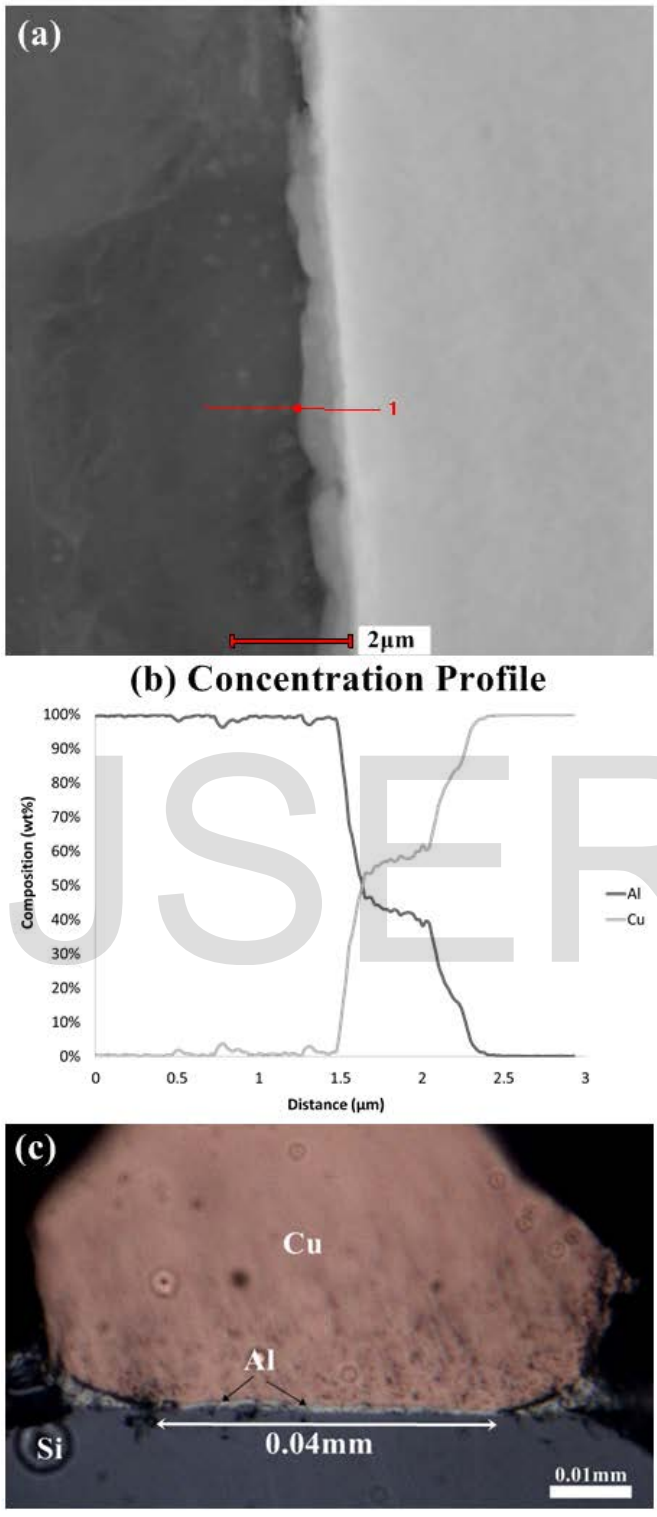

Figure 9: a) TEM image of Cu-Al bonding interface which was taken from the high stress area at the periphery of the bonding, (b) Concentration profile of Cu and Al elements along a red line across the bonding interface as defined in (a), (c) Optical microscopic image of Cu-Al bonding interface after mechanical cross-section.

REFERENCES

[1] Breach CD, Wulff FW. Microelectron Reliab 2010; 50:1.

[2] Kim H, Lee JY, Paik K, Koh K, Won J, Choe S, Lee J, Moon J, Park Y. IEEE Trans Components Packag Technol 2003;26:367.

[3] Charles A. Harper. Electronic Materials and Processes Handbook, 3rd ed. McGraw-Hill Professional; 2003.

[4] Xu H, Liu C, Silberschmidt V V, Wang H. Effects of Process Parameters on Bondability in Thermosonic Copper Ball Bonding, in: 2008 58th Electron. Components Technol. Conf. IEEE; 2008.

[5] Onuki J, Koizumi M, Araki I. IEEE Trans Components, Hybrids, Manuf Technol 1987;10:550.

[6] Yeoh LS. Characterization of Intermetallic Growth for Gold Bonding and Copper Bonding on Aluminum Metallization in Power Transistors, in: 2007 9th Electron. Packag. Technol. Conf. IEEE; 2007.

[7] Hang CJ, Wang CQ, Mayer M, Tian YH, Zhou Y, Wang HH. Microelectron Reliab 2008; 48:416.

[8] Xu H, Liu C, Silberschmidt VV. 2008 2nd Electron Syst Technol Conf 2008:891.

[9] Xu H, Liu C, Silberschmidt V V., Chen Z. J Electron Mater 2009;39:124.

[10] Na S, Hwang T, Park J, Kim J, Yoo H, Lee C. 2011 IEEE 61st Electron Components Technol Conf 2011:1740.

[11] Blish R, Li S, Kinoshita H, Morgan S, Myers A. Gold-Aluminum Intermetallic Formation Kinetics, in: 2006 IEEE Int. Reliab. Phys. Symp. Proc., vol. 1. IEEE; 2006.

[12] Funamizu Y, Watanabe K. Trans Japan Inst Met 1971; 12:147.

[13] Braunovic M, Alexandrov N. IEEE Trans Components, Packag Manuf Technol Part A 1994; 17:78.

[14] Wei TC, Daud AR. Microelectron Int 2002; 19:38.

[15] Wei TC, Daud AR. J Electron Packag 2003; 125:617.

[16] Lu D, Wong CP, editors. Materials for Advanced Packaging. Boston, MA: Springer US; 2009.

[17] Anand TJS, Chua KY, Lim BH. Mater Chem Phys 2012; 136:638.

[18] Bhattacharya SK. Experiments In Basic Electrical Engineering. New Age International; 2007.

[19] Anand TJS, Yau CK, Leong YS, Keat LW, Ting HM. Curr Appl Phys 2013; 13:1674.

[20] Kim D, Yoon J, Lee C, Jung S. Mater Trans 2003; 44:72.

[21] Breach CD, Wulff F, Tok CW. Microelectron Reliab 2006; 46:543.

[22] Breach CD, Wulff F. Microelectron Reliab 2004; 44:973.

[23] Abbasi M, Karimi Taheri a., Salehi MT. J Alloys Compd 2001; 319:233.

[24] Ho CY, Ackerman MW, Wu KY, Havill TN, Bogaard RH, Matula RA, Oh SG, James HM. J Phys Chem Ref Data 1983;12:183.

[25] Calister WD. Material Science and Engineering An Introduction, 6th ed. New York: John Wiley and Sons, Inc.; 2004.

[26] Murray JL. Int Met Rev 1985; 30:211.

[27] Rayne JA, Shearer MP, Bauer CL. Thin Solid Films 1980; 65:381.

[28] Zhou W, Liu L, Li B, Song Q, Wu P. J Electron Mater 2008;38:356.

[29] Cao S, Tirry W, Van Den Broek W, Schryvers D. J Microsc 2009;233:61.

[30] Volinsky A a, Rice L, Qin W, David Theodore N. Microelectron Eng 2004; 75:3.